The Internal Kink Mode in an Anisotropic Flowing Plasma with Application to Modeling Neutral Beam Injected Sawtoothing Discharges

J. P. Graves, O. Sauter

Centre de Recherches en Physique des Plasmas, Association EURATOM-Confédération Suisse,

EPFL, 1015 Lausanne, Switzerland

N. N. Gorelenkov

Princeton Plasma Physics Laboratory, Princeton, NJ, 08543, USA.

For some time it has not been clear to what extent neutral injected beam ions have a stabilizing influence on sawteeth. To investigate this, the well known toroidal internal kink instability is generalized to account for weakly anisotropic and flowing equilibria. An analytical approach is proposed, which upon employing an appropriate model distribution function, accurately accounts for the hot ion response of neutral beam injection (NBI) to the internal kink mode. Large fluid contributions, which are expected to arise as a consequence of the anisotropic velocity deposition of NBI, are identified and shown to be stabilizing to the internal kink mode for populations with large passing fractions. In particular for tangential injection, such as that employed in the Joint European Torus [J. Wesson, *Tokamaks*, 2nd ed. (Oxford Science Publications, Oxford, 1997), p. 581], it is found that fast ion stabilization can be dominated by anisotropic fluid effects rather than kinetic effects. In contrast, for predominantly trapped populations, the anisotropic fluid effects are destabilizing and thus reduce the stabilizing role of fast ions. This is especially evident for cases where the sub-sonic sheared toroidal plasma rotation induced by unbalanced NBI reduces kinetic stabilization. Sheared plasma rotation orientated either co or counter to the plasma current can reduce fast ion stabilization, but counter-rotation has the greatest effect by impeding the conservation of the third adiabatic invariant.

I. INTRODUCTION

The control of sawteeth is expected to be of paramount importance for a next step magnetically confined fusion device. The presence of highly energetic ions in large tokamaks has given rise to sawteeth with long quiescent times and large amplitudes [1] - [4]. Although this might seem to be an advance, large sawteeth also have detrimental ramifications. In particular, the radial location of the collapse event propagates with respect to the sawtooth quiescent time. The collapse radius has been predicted to be so large in the International Thermonuclear Experimental Reactor (ITER) [5] that coupling is likely to occur with instabilities located at other rational surfaces. Evidence of interaction between large sawteeth and 3/2 neoclassical tearing modes (NTM) has been observed [6] in the Joint European Torus (JET) [7], while discharges with smaller regular sawteeth are found to have increased core confinement, and are less likely to be coupled to confinement degrading NTM's. Hence it is seen that greater understanding and eventual control over the mechanisms that determine sawtooth stability is required. Key to this will be control over the interaction between fast minority ion dynamics and magnetohydrodynamic (MHD) stability.

This paper investigates the response of neutral beam injection (NBI) minority ions to the $m = n = 1$ internal kink mode. It is well known that NBI does not stabilize sawteeth as effectively as ion cyclotron resonance heating (ICRH). One important explanation for this [4] is that the minority ions of ICRH are more energetic than those of NBI and therefore conserve more readily the third adiabatic invariant Φ [8]. The latter requires that trapped ions complete many toroidal revolutions during the timescale of the mode so that the magnetic fluxes through the toroidal trajectories of the centers of these orbits are adiabatically conserved. However, other important differences between the heating schemes exist such as the variable degree of plasma rotation and anisotropy possible with NBI. Inclusion of the effect of anisotropy permits an investigation into the dependence of stability on the neutral beam injection angle, and enables comparisons with an existing treatment of anisotropic effects [9,10]. In addition, the effect of plasma rotation is important not least because strongly sheared profiles of up to 30 kHz have been measured in neutral beam plasmas in JET [11]. While the effect of such sub-sonic plasma flow on the MHD internal kink stability [12] is typically modest, the kinetic response [13] can be strongly modified. In particular, in the present paper it is seen that a large reduction in kinetic stabilization results from NBI ion orbits which do not adhere to the condition [4] for the conservation of Φ. This could help

to explain JET discharges [14] (e.g. discharge 8419) which show that the switching on of counter injected NBI coincides with much smaller and more irregular sawteeth than in the Ohmic phase. In contrast, similar discharges with co-injected beam ions typically give rise to sawteeth with periods up to 10 times that for Ohmic. More recent co injected NBI dischares in JET have been examined in detail [15] using the complete sawtooth model originally developed for the prediction of sawteeth in ITER [5]. The relatively large sawteeth, with periods of up to half a second, were shown to be principally due to the internal kink mode potential energy δW being above the threshold value of the resistive internal kink mode [16] for the duration of the sawtooth quiescent time. This further highlights the motivation of the present paper which seeks to improve the experimental relevance of the fast ion contribution to δW by incorporating anisotropy and plasma rotation.

In the following section, the stability analysis of the internal kink mode is generalized to account for an anisotropic and flowing equilibrium. Section III defines and normalizes a suitable model distribution function for NBI ions. The latter is applied to the hot ion kinetic and fluid terms, which, in the appendix, are greatly simplified and made numerically tractable. In Sec. IV typical JET parameters are chosen, and the fast ion contribution to the internal kink mode is evaluated numerically for differing NBI scenarios. Key to this will be variation of injection angle, focusing of pitch angle distribution, and toroidal rotation. The final section summarizes the results and discusses the implications.

II. HOT MINORITY ION CONTRIBUTION TO KINK MODE WITH ANISOTROPIC FLOWING EQUILIBRIUM

The modifications that hot ions bring to the internal kink mode have been documented many times. However, a consistent theoretical framework is presented here which includes equilibrium parameters that, although frequently ignored, exist in many experiments and are shown to significantly modify internal kink stability. In particular this section describes the effects of sheared plasma rotation and anisotropy on the internal kink mode, both of which arise as a consequence of NBI.

A. The internal Kink Mode in an anisotropic equilibrium

An equilibrium pressure exists which is described [17,18] by the double adiabatic model: $\underline{\underline{P}} = P_\perp \underline{\underline{I}} + (P_\| - P_\perp)\hat{\mathbf{e}}_\| \hat{\mathbf{e}}_\|$, where $\underline{\underline{I}}$ is the unit dyadic and $\hat{\mathbf{e}}_\|$ the unit vector parallel to the magnetic field. This pressure tensor comprises all particles in the plasma. If the equilibrium is perturbed by a MHD mode with displacement vector $\boldsymbol{\xi}$, a fluid 'f' potential energy term $\delta W_f = \frac{1}{2} \int d^3x\, \boldsymbol{\xi}^* \cdot (\boldsymbol{\nabla} \cdot \underline{\underline{\delta P}})$ arises as a consequence of a convective perturbation of the distribution function $\delta f = -\sum_j \boldsymbol{\xi} \cdot \boldsymbol{\nabla} F_j$, where j denotes a species distributed by $F_j(r, \mathcal{E}, \mu)$, $\mathcal{E} = v^2/2$ is the kinetic energy, $\mu = v_\perp^2/2B$ the magnetic moment and r the minor radius which is the label for the assumed circular flux surfaces. The remaining MHD energy terms are those due to perturbations in $\boldsymbol{j} \times \boldsymbol{B}$, where $\boldsymbol{j}$ is the current density and $\boldsymbol{B}$ the magnetic field. In a low beta plasma it can be shown that:

$$\delta W_f = -\frac{1}{2} \int d^3x\, \frac{\boldsymbol{\xi}^* \cdot \boldsymbol{\nabla} B}{B}(\delta P_\perp + \delta P_\|), \tag{1}$$

where

$$\delta P_\perp + \delta P_\| = -\xi_r \sum_j m_j \int dv^3 \left(\frac{v_\perp}{2} + v_\|\right) \frac{\partial F_j}{\partial r}. \tag{2}$$

Furthermore, by exploiting the invariance of $\mathcal{E}$ and μ:

$$\delta P_\perp + \delta P_\| = -\xi_r \left[\frac{\partial}{\partial r}(P_\perp + P_\|) - (P_\perp + P_\| + C)\frac{\partial}{\partial r}(\ln B)\right], \tag{3}$$

$$0 = \frac{\partial}{\partial \theta}(P_\perp + P_\|) - (P_\perp + P_\| + C)\frac{\partial}{\partial \theta}(\ln B), \tag{4}$$

where C is defined for example in Ref. [18] and θ is the poloidal angle.

At this point the principal perturbation $m = n = 1$ can be asserted. The variational analysis proceeds by writing the eigenfunction $\boldsymbol{\xi}$ and δW as a series expansion in the local inverse aspect ratio $\epsilon = r/R_0$, where r is the local minor radius and R_0 the axial major radius. Minimization of δW can then be undertaken order by order in ϵ^2. Equation (1) can be normalized so that it is formally $O(\epsilon^4)$ and hence does not interfere with the minimization of $O(\epsilon^2)$ energy terms. The latter identifies the leading order eigenfunction as top hat [19]. Employing $\int d^3x = 2\pi \oint d\theta \int_0^{r_1} dr\, r R^2/R_0$ and identifying ξ_r in Eqs. (1) and (3) with the top hat obtains:

$$\delta W_f = 2\pi^2 \xi_0^2 \int_0^{r_1} dr\, \epsilon \left[r \left\langle P_\perp + P_\| \right\rangle' + r \left\langle \left(P_\perp + P_\|\right) \cos 2\theta \right\rangle' + \right.$$
$$\left. R_0 \left\langle \left(P_\perp + P_\|\right) \cos \theta \right\rangle' + \frac{1}{2} \left\langle \left(P_\perp + P_\| + C\right)(1 + \cos 2\theta) \right\rangle + O(\epsilon P)\right], \tag{5}$$

4

where $' \equiv d/dr$, angular brackets denote poloidal orbit averaging, and r_1 is the radial position at which the safety factor $q(r)$ is unity. Also $B = B_0(1 - \epsilon \cos\theta)$ has been assumed. For isotropic distributed particles, the pressure components are not dependent on θ, and $P \equiv (P_\perp + P_\parallel)/2 = -C/2$, so that only the first term in Eq. (5) remains. However, this strongly destabilizing term, first highlighted by Shafranov [19], is exactly canceled for the $n = m = 1$ internal mode [20] when the effect of toroidicity in the $\boldsymbol{j} \times \boldsymbol{B}$ component of the perturbed force is taken into account. For an isotropic equilibrium, toroidal effects and where relevant flux surface shaping effects [21] are all that remain. The toroidal term [20] can be written in the form: $\delta W_T = \delta W_0 + \Delta'(r_1)\delta W_1 + (\Delta'(r_1))^2 \delta W_2$, where δW_0, δW_1 and δW_2 are functions of the q profile only, and can be obtained by solving driven Euler-Lagrange equations. Toroidal effects enter here through the local Shafranov shift gradient $\Delta'(r_1)$ which depends linearly on the poloidal beta $\beta_p = -(2\mu_0/B_0^2\epsilon_1^2 r_1^2) \int_0^{r_1} dr\, r^2 P'$. Here B_0 is the axial magnetic field and $\epsilon_1 = r_1/R_0$. On assuming anisotropy, the definition of $\Delta'(r_1)$ employed in δW_T should be modified to into account the poloidal dependence of $P_\perp$ and $P_\parallel$ [22,23]. However, it should be noted that it is not appropriate to use Bussac's formulation for δW_T in plasmas with a highly anisotropic equilibrium [23]. In particular if $P_\parallel/P_\perp \sim \epsilon$, the flux surfaces are found to be highly non-circular. This results in coupling of additional m, n harmonics and thus the standard equilibrium expansions employed for evaluation of toroidal [20] and shaping [21] effects are then invalid [22]. Nevertheless, it is usually only the hot minority ions that are anisotropically distributed, and for the NBI minority populations of interest in this paper, the corresponding hot pressure P_h is typically no greater than one third of the core bulk plasma P_c. Hence the approximate range of validity $\epsilon_1^{1/2} < P_\perp/P_\parallel < \epsilon_1^{-1/2}$ for Bussac's toroidal term should be met regardless of the hot ion distribution.

The third and fourth terms in Eq. (5) describe the effect of anisotropy on stability. The second term is negligible in all but extreme anisotropic cases. Hence it can be seen that δW_f can be separated into isotropic '0' and anisotropic 'A' parts to give $\delta W_f = \delta W_{f0} + \delta W_{fA}$ where approximately

$$\delta W_{f0} = -\pi \int_0^{r_1} dr\, r\epsilon \oint d\theta\, \xi_r^* \left(\delta P_\perp + \delta P_\parallel\right), \tag{6}$$

$$\delta W_{fA} = -\pi \int_0^{r_1} dr\, r \oint d\theta\, \xi_r^* \left(\delta P_\perp + \delta P_\parallel\right) \cos\theta. \tag{7}$$

Equations (7) and (6) arise from the leading order and first order expansion of $\int d^3x$ in ϵ respectively. In the following sections it is found that the anisotropic contribution to δW

5

is most conveniently expressed by Eq. (7) in conjunction with the general definition for $\delta P_\perp + \delta P_\parallel$ given by Eq. (2).

It is of interest to compare the anisotropic contribution to the internal kink mode with that obtained by Mikhailovskii [9,10]. If it is assumed that the poloidal dependence of $P_\perp + P_\parallel + C$ is weak such that $\left| \left(P_\perp + P_\parallel + C \right) / \left\langle P_\perp + P_\parallel + C \right\rangle - 1 \right| \ll 1$, then Eq. (4) yields $P_\perp + P_\parallel = \left\langle P_\perp + P_\parallel \right\rangle - \left\langle P_\perp + P_\parallel + C \right\rangle \epsilon \cos\theta$. Hence, for such an assumption Eq. (3) clearly realizes the perturbed pressure obtained by Mikhailovskii [24]: $\delta P_\perp + \delta P_\parallel = -\xi_r \left[\left\langle P_\perp + P_\parallel \right\rangle' - \epsilon \left\langle P_\perp + P_\parallel + C \right\rangle' \cos\theta \right]$. Substituting this into Eq. (6) merely yields Shafranov's cylindrical term as expected, while Eq. (7) is identified with the anisotropic contribution given in Ref. [10]:

$$\delta W_f^M = -\pi^2 \xi_0^2 \int_0^{r_1} dr\, r\epsilon \left\langle P_\parallel + P_\perp + C \right\rangle'. \tag{8}$$

This definition for the anisotropic modification to stability has been included more recently in an analysis of sawteeth in RF heated plasmas [25]. It is of interest to compare Eq. (8) with the generalized anisotropic contribution given by Eqs. (7) and (2). This is particularly important for minority heated plasmas since the hot 'h' ion pressure tensor typically depends strongly on θ, thus leading to inaccuracies in Eq. (8). In particular, since the core plasma is assumed to be isotropic, Eq. (8) is only valid if $\left| \left(P_{h\perp} + P_{h\parallel} + C_h \right) / \left\langle P_{h\perp} + P_{h\parallel} + C_h \right\rangle - 1 \right| \ll 1$. In fact, in general it is found that the latter identity is not met even for a distribution function which is only weakly anisotropic.

B. Hybrid Plasmas with a flowing equilibrium

For a hybrid plasma it is necessary to distinguish between quantities corresponding to hot minority ions, denoted by 'h', and the core plasma 'c' which comprises thermal ions and electrons. The leading order contributions to the toroidal plasma rotation arise from a finite thermal ion pressure gradient and from an equilibrium radial electric field E. It is appropriate to assume that poloidal flow is strongly damped [26], such that the toroidal rotation of the core plasma is given by:

$$\Omega = \Omega_E + \omega_{*pi}, \tag{9}$$

with

$$\Omega_E = \frac{qE}{B_0 r} \quad \text{and} \quad \omega_{*pi} = -\frac{qP_i'}{eZn_i B_0 r}. \tag{10}$$

Here eZ, n_i and P_i are respectively the charge, density and pressure of thermal ions. The common source of rotation for the different plasma species is that arising from the equilibrium electric field, i.e. Ω_E. For NBI scenarios, a mechanism can be envisaged whereby the momentum of the injected ions initially rotates the plasma, which in order to satisfy the force balance equation, establishes a large radial electric field. However, it is highlighted here that the toroidal rotation for impurity species is not measured to be the same as that of the core plasma [27,11]. The difference is expected to be of the order of the thermal ion diamagnetic frequency ω_{*pi} minus the corresponding quantity for the impurity species.

Before introducing the various contributions to the internal kink stability, it is appropriate to discuss the frequency regime of interest. For analyzing the hot ion response of 'sawtooth modes' with mode frequency ω, it is usually assumed that $\omega_{*h} \gg \omega$ and $\langle \omega_{mdh} \rangle \gg \omega$, where ω_{*h} and $\langle \omega_{mdh} \rangle$ are respectively the hot ion diamagnetic and bounce averaged magnetic drift frequencies. This is appropriate because, in contrast to 'fishbone modes', which generally satisfy [28] $\omega \sim \langle \omega_{mdh} \rangle$, sawteeth are believed to have mode frequencies of the order of ω_{*pi}. It has been pointed out [4] however that unlike ICRH scenarios, NBI heated plasmas do not always obey the following approximate condition for kinetic stabilization: $\omega_{*pi}/\langle \omega_{mdh} \rangle < 1$. This has been used to explain [4] why long sawteeth, of e.g. period $\tau \sim 1$ second in JET, are not frequently observed in NBI plasmas. In addition it may explain observation [29] of JET NBI discharges which display sawteeth in conjunction with fishbone-like activity. For this reason the effect of finite mode frequency on the kinetic contribution to the marginally stable potential energy is considered in the present paper, and conclusions are made about its affect in relation to low frequency sawtooth type modes.

For non-zero toroidal plasma rotation the mode frequency is Doppler shifted locally as follows [13]: $\omega \rightarrow \omega - \Omega_E(r)$. Providing the toroidal plasma velocity is much smaller than sonic speed, the internal kink dispersion relation can be written in terms of $\tilde{\omega} = \omega - \Omega_E(r_1)$ such that the toroidal rotation only appears in the kinetic contribution [13]. The present paper will be concerned with differential rotation $\Delta\Omega_E(r) = \Omega_E(r) - \Omega_E(r_1)$ of variable magnitude up to $\Delta\Omega_E \sim \langle \omega_{mdh} \rangle$. This of course requires that the injection of neutral beams is unbalanced. Upon retaining the mode frequency (in the plasma frame) $\tilde{\omega}$, the hot ion kinetic contribution to the internal kink is then:

$$\delta W_{hk} = -2^{5/2}\pi^3 m_h B_0 R_0 \left(\frac{\xi_0}{R_0}\right)^2 \int_0^{r_1} dr\, r \int_{1/B_{\max}}^{1/B_{\min}} d\alpha\, \frac{I_q^2}{K_b} \int_0^{\infty} d\mathcal{E}\, \mathcal{E}^{5/2} \frac{\partial F_h}{\partial \mathcal{E}} \left[\frac{\omega_{*h} + \Delta\Omega_E - \tilde{\omega}}{\langle \omega_{mdh} \rangle + \Delta\Omega_E - \tilde{\omega}}\right],$$

(11)

7

where F_h is the distribution function of hot ions which are assumed to have zero orbit width, $\alpha = \mu/\mathcal{E}$ is a pitch angle variable, and K_b and I_q are defined in the Appendix.

Conservation of the third adiabatic invariant, which has been shown to guarantee kinetic stabilization [4], is obtained for $\omega \ll n(\langle \omega_{mdh} \rangle + \Omega_E)$ in a plasma with an equilibrium electric field. The equivalent condition $\tilde{\omega} - \Delta\Omega_E \ll \langle \omega_{mdh} \rangle$ (with $n = 1$) is seen to be harder to satisfy for sheared rotation in the counter current direction ($\Delta\Omega_E < 0$) than for the static case. In contrast co-rotation assists in conserving the third adiabatic invariant. Close to marginal stability, evaluation of the dissipative contribution $\Im\{\delta W_{hk}\}$ can be employed to resolve the real part of the frequency $\tilde{\omega}$ of co-existing modes, and it is seen in Sec. IV B that a solution always exists with $\tilde{\omega} \sim \omega_{*pi}$ for which $\Re\{\delta W_{hk}\}$ is positive (stabilizing) over the range of plasma rotation considered. This therefore justifies the approach taken in the present paper whereby attention is primarily given to the reactive part of kinetic contribution $\Re\{\delta W_{hk}\}$ close to the stability threshold and with $\tilde{\omega} = 0$. The effect of plasma rotation induced by unbalanced injection, for which $\Delta\Omega_E \sim 3\omega_{*pi}$ is typical in JET, is more important than the effect of finite $\tilde{\omega}$ for the cases considered.

If the plasma is hot enough such that the effective ion-ion collision frequency satisfies $\nu_{ii} \ll \Delta\Omega_E$, the Kruskal-Oberman [30] limit applies for the kinetic response from thermal ions δW_{KO} [13]. This term is then independent of the diamagnetic, mode, precessional drift or toroidal rotation frequencies and is stabilizing for normal pressure profiles ($P' < 0$). The remaining potential energy terms of interest are the toroidal stability term δW_T [20], with the generalized expression for Δ' which takes into account the poloidal dependence of the pressure components [23], and the fluid term δW_{hf} which represents the anisotropic effects of hot ions. From Eqs. (7) and (2) it is seen that δW_{hf} is most conveniently defined in terms of the fast ion distribution function:

$$\delta W_{hf} = -\pi\xi_0^2 \int_0^{r_1} dr\, r \oint d\theta \, \cos\theta \int dv^3 \left(\frac{v_\perp}{2} + v_\parallel \right) m_h \frac{\partial F_h}{\partial r}. \tag{12}$$

Assuming that the mode does not lie inside the gap of the Alfvén continuum, the ideal stability criterion is given by $\delta W_T + \delta W_{KO} + \delta W_{hf} + \Re\{\delta W_{hk}\} > 0$. The remaining part of this paper is dedicated to analyzing the variation of the fast ion contribution to stability $\delta W_h = \delta W_{hf} + \Re\{\delta W_{hk}\}$ with respect to changing plasma rotation and distribution function.

III. THE FAST ION DISTRIBUTION FUNCTION

The fast ion distribution function that is appropriate for this study will be invariant to rapid gyro-motion and finite orbit widths. Thus it must be expressible in the form $F_h(\mathcal{E}, \mu, r)$, with kinetic energy $\mathcal{E} = v^2/2$, magnetic moment $\mu = v_\perp^2/2B$ and the minor radius r which defines the assumed circular flux surfaces.

The absolute velocity dependence of the NBI population is approximately described with a simple slowing down distribution $\sim 1/|v|^3$, such that $F_h \sim 1/\mathcal{E}^{3/2}$. However, the velocities of the minority ions are focused in the direction of injection. An analytical solution to the Fokker-Planck equation exists [31] which describes both the slowing down and the pitch angle scattering of the beam ions. A steady state approximation of the latter which has been employed in Ref. [32] to model the NBI distribution function is as follows:

$$F_h(\mathcal{E}, \mu, r) = \frac{c(r)}{\mathcal{E}^{3/2}} \exp[-(\lambda - \lambda_0)^2/\Delta\lambda^2] \tag{13}$$

for $0 \leq \mathcal{E} \leq \mathcal{E}_m$ and $F_h = 0$ for $\mathcal{E} > \mathcal{E}_m$. The pitch angle $\lambda = B_0\mu/\mathcal{E}$ is valid for $0 \leq \lambda \leq 1/(1-\epsilon)$. The parameter λ_0, which describes the mode (or central) pitch angle, is to leading order, defined in terms of the angle of injection χ from perpendicular as follows:

$$\lambda_0 \approx \cos^2 \chi. \tag{14}$$

Hence for perpendicular injection ($\chi = 0$) it is clear that $\lambda_0 \approx 1$, which indicates that the distribution function is peaked in trapped space, and vice-versa for azimuthal injection ($\chi = \pm\pi/2$). The spread of the distribution in the pitch angle is governed by the parameter $\Delta\lambda > 0$. For example, on letting $\Delta\lambda \to 0$, Eq. (13) becomes a delta function with discontinuity located at λ_0 such as that used by Chen *et al* [28] to model the effects of NBI on fishbones. The other extreme is $\Delta\lambda \gg 1$ which yields an isotropic distribution, independent of λ_0, such as that used [e.g. Refs. [33,34]] to analyze the effects of slowing-down alpha particles on the internal kink mode. It also is noted that the distribution function employed in Ref. [35] to model the effects of ICRH particles on sawteeth has a similar pitch angle dependence to that of Eq. (13).

It is possible to parameterize the distribution function of Eq. (13) by employing the results of TRANSP code [36]. In this code the Monte-Carlo routine computes the slowing down distribution function of the beam ions, so that such effects as pitch angle scattering and energy slowing down due to the background plasma are included. Equation (13) can then

be fitted to the computed distribution function to obtain the parameters λ_0 and $\Delta\lambda$. Figure 1 demonstrates this procedure for JET discharge 53595. In particular, while the central pitch angle is $\lambda_0 \approx 0.5$ for this discharge, the pitch angle width $\Delta\lambda$ exhibits a functional dependence in $\mathcal{E}$ and r. This is to be expected because preference in pitch angle will become less as the minority ions slow down due to collisions. However, for this paper, it is sufficient to employ an effective pitch angle width which is an average value over energy and radius. Hence, for discharge 53595 the effective pitch angle width is around $\Delta\lambda = 0.5$, and is in fact close to the actual width within the range $0 < r < r_1 \sim 0.4m$ and $40keV < \mathcal{E} < 80keV$. Thus the distribution function is simplified to enable evaluation of internal kink stability, but nevertheless the underlying physics remain. Namely that the distribution function is slowing down in energy, and Gaussian in pitch angle. The latter distribution identifies λ_0 and $\Delta\lambda^2$ with the mode and spread of the distribution in λ.

A. Distribution Function Normalization and Anisotropy

The coefficient $c(r)$ in Eq. (13) assumes the role of normalizing the distribution function. It is not possible to define $c(r)$ in terms of the hot ion density n_h without removing the singular behavior of Eq. (13) at small $\mathcal{E}$. An alternative is to retain this singular behavior but define $c(r)$ in terms of the hot ion pressure. A second parameter is the injection energy $\mathcal{E}_m$. The pressure related quantity chosen for normalizing the distribution function is $\langle P_h \rangle \equiv \left(\langle P_{h\perp} \rangle + \langle P_{h\parallel} \rangle \right)/2$ where angular brackets denote averaging over poloidal orbits of both passing and trapped particles.

For the distribution function of Eq. (13) it can be shown that $\langle P_{h\perp} \rangle = m_h 2^{3/2} \pi \mathcal{E}_m c(r) I_\perp$ and $\langle P_{h\parallel} \rangle = m_h 2^{3/2} \pi \mathcal{E}_m c(r) I_\parallel$, where $I_\perp$ and $I_\parallel$ describe the pitch angle and orbit integrals. The latter can be split into contributions from passing and trapped ions. Progress is made through a new pitch angle k^2 which for trapped ions is defined $k^2 = (1 - \alpha B_0(1 - \epsilon))/2\alpha B_0\epsilon$ and for passing ions $k^2 = 2\alpha B_0/(1 - \alpha B_0(1 - \epsilon))$. Integrating in poloidal angle and pitch angle obtains $c(r) = \langle P_h \rangle \big/ \left[2^{1/2} \pi m_h \mathcal{E}_m \left(I_\perp(r) + I_\parallel(r) \right) \right]$ with

$$I_\perp(r) = \frac{2}{\pi}(2\epsilon)^{1/2} \int_0^1 dk^2 \left(\frac{K(k^2)f_1(k^2, \epsilon)}{[1 + \epsilon(2k^2 - 1)]^{5/2}} + \frac{k^2 K(k^2)f_2(k^2, \epsilon)}{[k^2 + \epsilon(2 - k^2)]^{5/2}} \right), \qquad (15)$$

$$I_\parallel(r) = \frac{4}{\pi}(2\epsilon)^{3/2} \int_0^1 dk^2 \left(\frac{[E(k^2) + (k^2 - 1)K(k^2)]f_1(k^2, \epsilon)}{[1 + \epsilon(2k^2 - 1)]^{5/2}} + \frac{E(k^2)f_2(k^2, \epsilon)}{[k^2 + \epsilon(2 - k^2)]^{5/2}} \right), \quad (16)$$

where

$$f_1 = \exp\left[-\left|\frac{1}{1 + \epsilon(2k^2 - 1)} - \lambda_0\right|^2 / \Delta\lambda^2\right] \quad \text{and} \quad f_2 = \exp\left[-\left|\frac{k^2}{k^2 + \epsilon(2 - k^2)} - \lambda_0\right|^2 / \Delta\lambda^2\right].$$

(17)

$I_\perp$ and $I_\parallel$ are formally of order ϵ^0 and converge as $\epsilon \to 0$. In the isotropic limit, such that f_1 and f_2 of Eqs. (17) are unity, it can be shown that $I_\perp + I_\parallel = 8/3$ and $I_\perp/I_\parallel = \langle P_{\perp h}\rangle / \langle P_{\parallel h}\rangle = 1$ for vanishing ϵ. However, in general Eqs. (15) - (16) must be evaluated numerically for varying r since $I_\perp$ and $I_\parallel$ are defined in terms of $K(k^2)$ and $E(k^2)$, complete elliptic integrals of the first and second kind [37] respectively.

In addition to normalizing the distribution function, $I_\perp$ and $I_\parallel$ also permit straightforward calculation of the following macroscopic measure of the anisotropy:

$$A_h \equiv \langle P_{h\perp}\rangle / \langle P_{h\parallel}\rangle = I_\perp/I_\parallel.$$

Figure 2 plots A_h versus the pitch angle width $\Delta\lambda$ for different central pitch angles λ_0. It can be seen that the isotropic limit is rapidly reached for $\Delta\lambda > 2$ regardless of λ_0, while $A_h \sim 10$ or $\sim 1/10$ can be obtained for sufficiently small pitch angle width ($\Delta\lambda \sim 0.15$) and $\lambda_0 > 0.9$ or $\lambda_0 < 0.2$ respectively. For JET discharge 53595, for which $\Delta\lambda \approx 0.5$ and $\lambda_0 = 0.5$, the anisotropy is $A_h \approx 0.7$.

B. Regions of poor/good curvature and the poloidal dependence of $P_{h\perp}$ and $P_{h\parallel}$

Another measure of anisotropy which is sensitive to changes in $\Delta\lambda$ and λ_0 is the trapped - passing fraction. This definition, which is related to but not the same as A_h, is important because only trapped ions contribute to the kinetic modification of the internal kink mode. In addition, trapped particles exist in the region of poor curvature and as a result are seen to be destabilizing to the fluid contribution to the kink mode, while passing ions are stabilizing.

The role of passing and trapped ions on fluid stability can be observed by examining the poloidal dependence of the hot ion pressure components. The appropriate moments of the distribution function of Eq. (13) can be easily evaluated to obtain $P_{h\parallel}(\epsilon, \theta)$, $P_{h\perp}(\epsilon, \theta)$ and $C_h(\epsilon, \theta)$ for differing λ_0 and $\Delta\lambda$. Figure 3 shows a polar plot of $P_h = (P_{h\parallel} + P_{h\perp})/2$, where the angular variable is the poloidal angle. Also shown is Mikhailovskii's [10,24] approximated form of the hot pressure $P_h^M = \langle P_h\rangle - \langle (P_{h\perp} + P_{h\parallel} + C_h)/2\rangle \epsilon \cos\theta$ which is used in Eq. (8)

11

for the hot ion anisotropic term δW_{hf}^M. The chosen local inverse aspect ratio $\epsilon = 0.45/3$ is typical of that near the $q = 1$ surface in JET and the pitch angle width $\Delta\lambda = 0.5$ reflects the TRANSP simulations of JET. Figure 3(a) is for an injection angle of $\chi = 14°$, for which $\lambda_0 = 0.94$ and $A_h = 2.14$. It can be seen that P_h and P_h^M are shifted almost identically toward the outboard side. This has occurred because of the increased number of trapped particles which exist in the outer region of poor curvature. Figure 3(b) is for an injection angle of $\chi = 30°$, for which $\lambda_0 = 0.75$. Since the corresponding anisotropy $A_h = 1.44$ it might be expected that Fig. 3(b) would reflect a similar but smaller destabilizing shift to that of Fig. 3(a). This is observed in the plot of P_h^M, but not the plot of P_h which correctly displays a small shift toward the stabilizing region of good curvature. Finally Fig. 3(c) is for a typical JET injection angle of $\chi = 45°$, for which $\lambda_0 = 0.5$ and $A_h = 0.8$. The plot of P_h shows a strongly stabilizing shift toward the inboard side, while P_h^M displays only a small stabilizing shift.

The reason for the difference between $P_h(\theta)$ and $P_h^M(\theta)$ can be resolved by evaluating $\left|\left(P_{h\perp} + P_{h\parallel} + C_h\right)/\left\langle P_{h\perp} + P_{h\parallel} + C_h\right\rangle - 1\right|$. The latter quantity must be much less than unity for P_h^M to be a valid approximation of P_h. This means that the poloidal variation of $P_{h\perp} + P_{h\parallel} + C_h$ must be weak compared to its mean value. However, it is seen that $P_{h\perp} + P_{h\parallel} + C_h$ is only non-zero if the distribution function is anisotropic, and hence its poloidal variation is necessarily leading order. Upon choosing $\epsilon = 0.45/3$ and $\lambda_0 = 0.5$ it is found that $\left(P_{h\perp} + P_{h\parallel} + C_h\right)/\left\langle P_{h\perp} + P_{h\parallel} + C_h\right\rangle - 1$ varies approximately between ± 0.6 over $0 < \theta < 2\pi$. This result is valid for arbitrarily large $\Delta\lambda$, and therefore A_h arbitrarily close to unity.

C. Analytical Forms of Hot ion contribution to δW

In this section analytical forms are developed for the various hot ion contributions to the internal kink mode. The energy integrals can be evaluated analytically on assuming the distribution function of Eq. (13), thus allowing hot δW terms to be calculated through nested numerical integration in radius and pitch angle. The potential energy terms comprise the sum of kinetic 'k' and fluid 'f' components: $\delta W_h = \delta W_{hk} + \delta W_{hf}$. Each of these are defined in such a way as to facilitate numerical evaluation of stability.

The normalized potential energy terms $\delta \hat{W} = \delta W/(6\pi^2 R_0 \xi_0^2 \epsilon_1^4 B_0^2/\mu_0)$ are now evaluated. Inserting the distribution function of Eq. (13) into Eq. (A12) reveals the following hot kinetic

term:

$$\delta\hat{W}_{hk} = -\frac{2^{5/2}}{3\pi\epsilon_1^4 R_0^{3/2}}\left(\frac{\mu_0}{B_0^2}\right)\int_0^{r_1} dr\, r^{3/2}\left(\frac{\langle P_h\rangle}{I_\parallel + I_\perp}\right)'\int_0^1 dk^2\frac{\mathcal{F}_q^2\, f_1(\epsilon, k^2)}{K(k^2)[\mathcal{F}_1 + 2s\mathcal{F}_2 - \eta(1/4q^2 + \mathcal{F}_3)]}\times$$

$$\left\{1 - (\Delta\Omega_E - \tilde{\omega})\ln\left[1 + \frac{\langle\omega_{mdh}(\mathcal{E}_m)\rangle}{\Delta\Omega_E - \tilde{\omega}}\right]\left(\frac{reZ_h B_0}{qm_h\mathcal{E}_m}\right)\left[\frac{R_0}{\mathcal{F}_1 + 2s\mathcal{F}_2 - \eta(1/4q^2 + \mathcal{F}_3)} + \frac{3}{2\left[\ln\left(\frac{\langle P_h\rangle}{I_\parallel + I_\perp}\right)\right]'}\right]\right\} \quad (18)$$

where $f_1(\epsilon, k^2)$ is defined in Eq. (17) and $\langle\omega_{mdh}(\mathcal{E}_m)\rangle$ is the magnetic drift precession, defined in Eq. (A14), evaluated at injection energy $\mathcal{E} = \mathcal{E}_m$. Note that Eq. (18) contains a Landau resonance if $1 + \langle\omega_{mdh}(\mathcal{E}_m)\rangle/(\Delta\Omega_E - \tilde{\omega}) < 0$ within the range of nested integration. Thus a frequency resonance, which is described by $\Delta\Omega_E + \langle\omega_{mdh}\rangle - \tilde{\omega} = 0$, exists for some energy $0 < \mathcal{E} < \mathcal{E}_m$ and within a certain range of pitch angle and radius. This resonance condition describes [13] mode-particle matching of the kink mode frequency in the laboratory frame ω with the total toroidal drift precession of trapped ions which includes the contribution from an equilibrium electric field $\langle\omega_{dh}\rangle = \langle\omega_{mdh}\rangle + \Omega_E(r)$.

As a consequence of the possible Landau resonance in δW_{hk}, Eq. (18) contains both real and imaginary parts. $\Re\{\delta\hat{W}_{hk}\}$ and $\Im\{\delta\hat{W}_{hk}\}$ are identified close to marginal stability (i.e. $\Im\{\tilde{\omega}\}$) by testing the sign of $1 + \langle\omega_{mdh}(\mathcal{E}_m)\rangle/(\Delta\Omega_E - \tilde{\omega})$ throughout the range of nested integration and using the property $\ln(-|x|) = \ln(|x|) + i\pi$. Note however that fast ion stability is principally governed by $\Re\{\delta W_h\}$ for the low frequency sawtooth modes of interest here. Therefore for convenience $\delta\hat{W}_h$ and $\delta\hat{W}_{hk}$ henceforth denote $\Re\{\delta\hat{W}_h\}$ and $\Re\{\delta\hat{W}_{hk}\}$ respectively.

The fluid contribution δW_{hf} is most conveniently defined in the form of Eq. (12). The appendix derives an analytical simplification which involves treating separately the trapped component δW_{hf}^t and passing component δW_{hf}^p of $\delta W_{hf} = \delta W_{hf}^t + \delta W_{hf}^p$. Inserting Eq. (13) into Eq. (A4) yields

$$\delta\hat{W}_{hf}^t = \frac{2^{5/2}}{3\pi\epsilon_1^4 R_0^{3/2}}\left(\frac{\mu_0}{B_0^2}\right)\int_0^{r_1} dr\, r^{3/2}\left(\frac{\langle P_h\rangle}{I_\parallel + I_\perp}\right)'\int_0^1 dk^2\frac{2G_1^t(\epsilon, k^2) + G_2^t(\epsilon, k^2)}{[1 + \epsilon(2k^2 - 1)]^{5/2}}f_1(\epsilon, k^2), \quad (19)$$

where Eqs. (A6) and (A7) G_1^t and G_2^t. The passing-fluid response of Eq. (A8) becomes

$$\delta\hat{W}_{hf}^p = \frac{2^{5/2}}{3\pi\epsilon_1^4 R_0^{3/2}}\left(\frac{\mu_0}{B_0^2}\right)\int_0^{r_1} dr\, r^{3/2}\left(\frac{\langle P_h\rangle}{I_\parallel + I_\perp}\right)'\int_0^1 dk^2\frac{2G_1^p(\epsilon, k^2) + G_2^p(\epsilon, k^2)}{[k^2 + \epsilon(2 - k^2)]^{5/2}}f_2(\epsilon, k^2), \quad (20)$$

where the pitch angle y^2 has been relabeled as k^2 in the definition of G_1^p and G_2^p given in Eqs. (A10) and (A11). The functional form of $2G_1^p + G_2^p$ used here is exact, and due to a

great deal of cancellation, is not singular for vanishing k^2. Instead $2G_1^p + G_2^p = -\pi\epsilon^2$ as $k^2 \to 0$.

Finally Mikhailovskii's [10] anisotropic term is defined in terms of the model NBI distribution function. Equations (8), (13) and (A1) yield

$$\delta\hat{W}_h^M = \frac{2}{3R_0^2\epsilon_1^4}\left(\frac{\mu_0}{B_0^2}\right)\left[\int_0^{r_1} dr\, r\, \langle P_h \rangle \Delta_C - \frac{r_1^2}{2}\langle P_h(r_1) \rangle \Delta_C(r_1)\right], \qquad (21)$$

with $\Delta_C = 1 - \frac{5}{2}\left(\frac{I_c}{I_\perp + I_\parallel}\right)$ and

$$I_c = (2\epsilon)^{1/2}\frac{2}{\pi}\int_0^1 dk^2\, K(k^2)\left[\frac{f_1(\epsilon, k^2)}{[1 + \epsilon(2k^2 - 1)]^{7/2}} + \frac{k^4 f_2(\epsilon, k^2)}{[k^2 + \epsilon(2 - k^2)]^{7/2}}\right]. \qquad (22)$$

Δ_C is zero for an isotropic distribution. For an anisotropic distribution Δ_C is limited in magnitude as follows. For $A_h \equiv \langle P_{h\perp} \rangle / \langle P_{h\parallel} \rangle \to 0$, which corresponds to $\lambda_0 \to 0$ and $\Delta\lambda \to 0$, it is found that $\Delta_C = 1$. This agrees with the result given by Mikhailovskii in Eq. (4.18) of Ref. [9]. Furthermore, $\Delta_C = -1$ is obtained for $1/A_h \to 0$, which corresponds to $\lambda_0 \to 1$ and $\Delta\lambda \to 0$. This identity limits the destabilizing effect of $\delta\hat{W}_h^M$ for predominantly trapped distributions and therefore differs greatly from the corresponding limit given by Eq. (4.18) of Ref. [9].

IV. STABILITY OF THE INTERNAL KINK FOR NBI SCENARIOS

In this section the stability of the internal kink mode is determined for various NBI scenarios. Key to this will be quantifying the possible destabilizing effects of toroidal rotation and anisotropy. The following profiles and parameters typical for JET equilibria are used: $a = 1.25$m, $R_0 = 3$m, $B_0 = 3$T. The safety factor profile is $q = q_0(1 + \lambda_q(r/a)^{2\nu_q})^{1/\nu_q}$ with $q_0 \equiv q(0) = 0.75$, $\lambda_q = 22.6$ and $\nu_q = 1.74$ which gives $r_1/a = 0.36$ and $q_a = 4.6$. The poloidal averaged pressure profile for the hot ions is given by $\langle P_h \rangle = P_{h0}[1 - (r/a)^2]^2$ with P_{h0} the central pressure. This profile represents well the TRANSP simulations. It is possible to write $P_{h0} = e\, n_{h0}T_{h0}$, where e is the absolute charge of the electron, n_{h0} is the density of hot ions and T_{h0} the corresponding temperature (units of electron volts) for a Maxwellian distribution. Quantities chosen here are $n_{h0} = 0.135 \times 10^{19}/m^3$ and $T_{h0} = 80$ keV. Such a temperature corresponds to that produced by the Octant 4 NBI system in JET. Note that although the anisotropy is varied in the following sections, $P_h(r) = \langle P_{h\perp} + P_{h\parallel} \rangle / 2$ remains constant throughout. The injection energy $\mathcal{E}_m$ arrives from the property $m_h\mathcal{E}_m/eT_{h0}(eV) \sim$

14

1. Hence $m_h \mathcal{E}_m / e = 80$ keV is used in this paper. The charge coefficient Z_h is chosen to be unity, i.e. either hydrogen or deuterium is assumed.

The pressure profile of the core plasma modifies δW_h through η, a parameter of the magnetic precession frequency given in Eq. (A14). The core plasma pressure profile assumed is $P_c = P_{c0}[1 - (r/a)^2]^3$, where $P_{c0} = e(n_{i0}T_{i0} + n_{e0}T_{e0})$, with $n_{i0} = n_{e0} = 4 \times 10^{19}$ and $T_{i0} = T_{e0} = 4.5$keV. Hence the ratio of the core pressure and hot ion pressure

$$Q = P_c / P_h$$

is 10/3 in the center, which is a typical value for NBI experiments. In addition, it will be seen later that for this choice of total pressure profile and the above q profile, Bussac's [20] toroidal term is very small such that ideal stability is largely determined by δW_h.

The toroidal rotation profile which accurately fits the data of Ref. [11] is

$$\Omega_E(r) = \Omega_{E0}\left[1 - \left(\frac{r}{a}\right)^2\right]^{3/2} .$$

Hence for the parameters chosen, the differential rotation $\Delta\Omega_E(r) = \Omega_E(r) - \Omega_E(r_1)$ at the center is $\Delta\Omega_E(0) \approx 0.2\,\Omega_{E0}$. The magnitude of the central toroidal rotation Ω_{E0} is a parameter which, in the forthcoming analysis, will be varied as $-40\,\text{kHz} < \Omega_{E0} < 40\,\text{kHz}$. Such a range is relevant for JET where toroidal rotation frequencies of up to 30 kHz have been measured in recent NBI experiments [11]. The other parameters that will be varied concern those that govern the pitch angle dependence of the distribution function. Although λ_0 and $\Delta\lambda$ are both measured and simulated to be around 0.5 in JET, it is of interest to see how the stability of the internal kink mode can change with respect to different injection scenarios. The central pitch angle λ_0 will be varied by changing the injection angle χ according to Eq. (14). In addition, since the transfer of momentum from the minority ions to the plasma gives rise to the $E \times B$ component of the toroidal rotation, the injection angle and Ω_{E0} cannot be totally independent. In particular, counter-injection gives rise to rotation in the opposite direction to co-rotation and balanced injection (co and counter) yields no measurable rotation [27]. However, the functional dependence of Ω_{E0} with χ is not at all clear because of such important issues as the change in the deposition of injected ions with χ. Hence, in Sec. IV B the toroidal rotation and injection angle are treated as independent parameters.

A. The Effect of Anisotropy on Stability

In this section the stability of the internal kink mode is evaluated for differing NBI scenarios. In particular, the dependence of stability on injection angle and pitch angle width is examined. The effects of finite plasma rotation and mode frequency are treated in Sec. IV B, while in the present section $\tilde{\omega} = 0$ and $\Delta\Omega_E = 0$ is employed.

Figure 4 plots $\delta\hat{W}_{hf}$, $\delta\hat{W}_{hk}$ and $\delta\hat{W}_h = \delta\hat{W}_{hf} + \delta\hat{W}_{hk}$ and $\delta\hat{W}_{hf}^M$ with respect to $\Delta\lambda$ for two different χ. In Fig. 4(a), for which $\chi = 45°$ ($\lambda_0 = 0.5$), it can be seen that $\delta\hat{W}_{hk}$ increases monotonically from zero with respect to $\Delta\lambda$. This can be explained by the fact that for $\lambda_0 = 0.5$ the number of trapped ions increases monotonically again from zero with respect to $\Delta\lambda$. The majority of ions are passing for $\Delta\lambda < 0.5$ and hence $\delta\hat{W}_{hf}$ is large and positive. As expected, the latter quantity decreases toward zero as $\Delta\lambda$ increases, i.e. as the distribution function approaches isotropy. The figure shows that the fluid effects are strongly stabilizing to the kink mode for $\chi = 45°$. For the example typical of JET ($\lambda_0 = 0.5$ and $\Delta\lambda = 0.5$) it can be seen that $\delta\hat{W}_{hf} \approx \delta\hat{W}_{hk}$ which suggests the importance of passing ions, heated by NBI, for sawtooth stabilization in JET. Earlier attempts [15,32] to quantify the effect of NBI ions on the internal kink mode did not include anisotropic fluid effects. Hence from Refs. [15,32] it would be concluded that for the NBI angle of injection in JET the fast ion stabilization diminishes as $\Delta\lambda \to 0$. The similarity between Fig. 2 of Ref. [32], Fig. 2 of Ref. [15] and the kinetic component of Fig. 4(a) is clear. However, it is now seen that the net result of including kinetic and anisotropic fluid effects is that $\delta\hat{W}_h$ varies only marginally with respect to $\Delta\lambda$. It is interesting to note that $\delta\hat{W}_{hf}^M$ is a factor of three smaller than $\delta\hat{W}_{hf}$. This remains true as $\Delta\lambda \to \infty$, which as observed in Fig. 3(c), occurs because the approximated form of the hot pressure $P_h^M(\theta, r)$ is not deformed sufficiently toward the stabilizing region of good curvature.

The curves in Fig. 4(b) are for the near perpendicular injection angle of $\chi = 14°$. This is comparable to the injection angle employed in the Poloidal Divertor Experiments (PDX) [38] where co and counter beam injection gave rise to contrasting sawtooth and fishbone characteristics. The corresponding central pitch angle $\lambda_0 = 0.94$. For $\Delta\lambda < 0.5$, the anisotropy $A_h > 2$ which indicates that the majority of the hot ions are trapped. As expected $\delta\hat{W}_{hf}$ is increasingly destabilizing for reducing $\Delta\lambda$. It is seen that the destabilizing fluid effects that result from strongly trapped populations almost balances the corresponding increased kinetic stability. Hence, as also observed for $\chi = 45°$, hot ion stability does not

16

vary greatly with respect to $\Delta\lambda$. In addition, it is interesting to note that for this choice of injection angle it is found that $\delta\hat{W}_{hf}^{M} \approx \delta\hat{W}_{hf}$. This can be understood by observing Fig. 3(a) which shows that $P_h(\theta)$ and $P_h^{M}(\theta)$ are shifted almost identically toward the region of poor curvature.

Figure 5(a) shows $\delta\hat{W}_h$, $\delta\hat{W}_{hk}$, $\delta\hat{W}_{hf}$ and $\delta\hat{W}_{hf}^{M}$ as a function of χ for $\Delta\lambda = 0.5$. The plot shows that the stability threshold for $\delta\hat{W}_{hf}$ is approximately $\chi = 25°$, while the stability threshold of $\delta\hat{W}_{hf}^{M}$ is approximately $40°$. This can be understood upon observation of Fig. 3(b) which illustrates a stabilizing shift of $P_h(\theta)$ and destabilizing shift of $P_h^{M}(\theta)$ for $\chi = 30°$. Figure 5(a) shows that the anisotropic fluid contribution $\delta\hat{W}_{hf}$ is increasingly stable and the kinetic contribution vanishes as injection approaches the azimuthal direction. Hence it is seen that hot ion stability varies only moderately with respect to injection angle or indeed with respect to the corresponding degree of anisotropy A_h which is depicted in Fig. 5(b). It is also possible to evaluate the anisotropy A corresponding to the entire plasma (thermal ions, electrons and hot ions):

$$A \equiv \frac{P_c + \langle P_{h\perp} \rangle}{P_c + \langle P_{h\parallel} \rangle} = \frac{Q(1 + A_h) + 2A_h}{Q(1 + A_h) + 2}.$$

Given that $Q = 10/3$ for the chosen equilibrium, the approximate range of plasma anisotropy corresponding to Figure 5 is $0.75 < A < 1.25$. As discussed in Sec II, for such a small range of anisotropy the effect on the toroidal contribution δW_T of the resulting slightly shaped surfaces is ignorable [22]. Hence, also ignoring the collisionless kinetic contribution from thermal ions, the stability of ideal internal kink mode is accurately given by $\delta\hat{W} = \delta\hat{W}_T + \delta\hat{W}_h$, where $\delta\hat{W}_T$ is the well known toroidal term of for example Bussac et al [20]. Numerically evaluating the driven Euler-Lagrange equations to obtain b and c of Ref. [20] for the chosen q profile and including the entire pressure for evaluation of β_p ($= 0.141$) obtains $\delta\hat{W}_T = -0.00066$. The safety factor, β_p and thus $\delta\hat{W}_T$ are fixed throughout the numerical analysis in this section and the next. Hence, for the chosen parameters, ideal stability is almost entirely governed by $\delta\hat{W}_h$.

B. Combined Effects of Toroidal Rotation and Anisotropy on Stability

In this section the effect of plasma rotation is included in the stability calculations of the internal kink mode. Initially the real and imaginary kinetic contributions $\Re\{\delta\hat{W}_{hk}\}$ and $\Im\{\delta\hat{W}_{hk}\}$ are plotted over an unrealistically large range of Ω_{E0} for an isotropic distribution

function. Figure 6 yields the characteristic kinetic response of the fast ions for (a) $\tilde{\omega} = 0$ and (b) $\tilde{\omega} = 1$ kHz. For all cases the mode is taken to be close to marginal stability, i.e. $\Im\{\tilde{\omega}\} = 0$ is assumed. The imaginary contribution $\Im\{\delta\hat{W}_{hk}\}$ quantifies the collisionless Landau energy transfer due to resonance between the toroidal orbits of the trapped ions and the kink mode. Recall that the mode frequency ω is Doppler shifted to $\omega - \Omega_E(r)$ such that the resonance condition is given by $\langle\omega_{mdh}\rangle + \Delta\Omega_E - \tilde{\omega} = 0$, where $\tilde{\omega} = \omega - \Omega_E(r_1)$. The peak in $\Im\{\delta\hat{W}_{hk}\}$ occurs where the deeply trapped ions with maximum energy $\mathcal{E}_m$ resonate with the mode. The corresponding magnetic precession frequency $\langle\omega_{mdh}\rangle$ for the parameters chosen at the beginning of Sec. IV is approximately 6 kHz close to r_1. In addition, the real contribution $\Re\{\delta\hat{W}_{hk}\}$, which contains the principal part of the simple pole singularity, is approximately a minimum where $\Im\{\delta\hat{W}_{hk}\}$ is largest.

Let us first consider the $\tilde{\omega} = 0$ case shown in Fig. 6 (a). The peak in $\Im\{\delta\hat{W}_{hk}\}$ and minimum in $\Re\{\delta\hat{W}_{hk}\}$ occurs for counter-rotation of $\Omega_{E0} = 5\Delta\Omega_E(0) \sim 30$ kHz. For co-rotation, resonance can only occur for reverse magnetically precessing ions ($\langle\omega_{mdh}\rangle < 0$). Since there are not many of these $\Im\{\delta\hat{W}_{hk}\}$ reduces to zero very quickly for increased co-rotation. Meanwhile $\Re\{\delta\hat{W}_{hk}\}$, which determines the kinetic contribution to stability in the marginal case, is peaked close to $\Omega_{E0} = 0$ and reduces for increased co-rotation. This can be understood by noting that $(\omega_{*h} + \Delta\Omega_E)/(\langle\omega_{mdh}\rangle + \Delta\Omega_E)$ decreases from $\sim \epsilon^{-1}$ to ~ 1 as $\Delta\Omega_E$ is increased from zero to a frequency much greater than $\langle\omega_{mdh}\rangle$.

Now let us consider the $\tilde{\omega} = 1$ kHz case shown in Fig. 6 (b). Close to marginal stability the imaginary part of the ideal dispersion relation [e.g. [39]] resolves the real mode frequency $|\tilde{\omega}| = 3^{1/2}\pi\epsilon_1^2\omega_A\Im\{\delta\hat{W}_{hk}\}/s_1$, where $\omega_A = v_A/R_0$ is toroidal Alfvén frequency. Given the magnitude of $\Im\{\delta\hat{W}_{hk}\}$ in Fig. 6(a) or (b) and the parameter values defined at the beginning of Sec IV, it is found that $|\tilde{\omega}| < 0.8$ kHz. If finite Larmor radius effects (FLR) are now included, the imaginary part of the ideal dispersion relation is modified to $[\tilde{\omega}(\tilde{\omega} - \omega_{*pi})]^{1/2} = 3^{1/2}\pi\epsilon_1^2\omega_A\Im\{\delta\hat{W}_{hk}\}/s_1$, where $\omega_{*pi} = 0.77$ kHz for the typical JET plasma parameters chosen. A solution therefore exists in the Alfvén continuum with ordering $\tilde{\omega} \sim \omega_{*pi} \sim 1$ kHz for which $\Re\{\delta W_{hk}\}$ is stabilizing over the range of plasma rotation. It is seen that inclusion of finite $\tilde{\omega}$ does not significantly modify the kinetic contribution to the stability threshold, which is governed by $\Re\{\delta\hat{W}_{hk}\}$. This is demonstrated in Fig. 6(b) where a finite mode frequency of $\tilde{\omega} = 1$ kHz is seen to merely shift the curve of $\Re\{\delta\hat{W}_{hk}\}$ in Fig. 6(a) to the right by approximately $\tilde{\omega}[\Omega_{E0}/\Delta_E(0)] = 5$ kHz. In contrast, the curves of $\Im\{\delta\hat{W}_{hk}\}$ in Fig. 6(a) and (b) differ significantly for co-rotation. This follows because close

to r_1, where $\Delta\Omega_E \approx 0$, Landau resonance arises from forward magnetically precessing ions with frequency $\approx \tilde{\omega} = 1$ kHz. Such ions are much more numerous than the static or reverse precessing ions which provide the Landau resonance exhibited in Fig. 6(a) for $\Omega_{E0} > 0$.

Figure 7 shows $\delta\hat{W}_h$ with respect to a realistic range of central toroidal plasma rotation. The mode frequency $\tilde{\omega}$ has been set to zero. Figure 7(a) is for an injection angle of $45°$. The broad pitch angle width of $\Delta\lambda = 2$ approximately reproduces the plot of $\Re\{\delta\hat{W}_{hk}\}$ in Fig. 6(a). It is seen that counter-rotation of -30 kHz reduces $\delta\hat{W}_h$ by more than a factor of two. Co-rotation of 30 kHz also reduces $\delta\hat{W}_h$ but not by as much as counter rotation. The sensitive dependence of kink mode stability on plasma rotation weakens for decreasing $\Delta\lambda$ since $\delta\hat{W}_h$ is then increasingly dominated by $\delta\hat{W}_{hf}$; a quantity independent of toroidal rotation. In contrast Fig. 7(b), which is for $\chi = 14°$, shows that the variation of $\Re\{\delta\hat{W}_h\}$ with respect to changing plasma rotation is increasingly sensitive for decreasing $\Delta\lambda$. This follows because the fluid contribution is destabilizing, such that the variation of $\Re\{\delta\hat{W}_{hk}\}$ with respect to co and counter plasma rotation gives rise to an even greater variation in $\Re\{\delta\hat{W}_h\}$. This trend is amplified as $\Delta\lambda$ is reduced.

Finally, it is interesting to compare Figures 4 - 7 with $\delta\hat{W}_h = 0.0056$ which for the chosen parameters, is obtained with the simplified analytical model employed in Ref. [5] for slowing down alphas and Ref. [15] for NBI ions. Note that the kinetic term defined in Ref. [5] has been multiplied by $2^{1/2}$ so that it matches the correct expression given in Ref. [15]. It can be seen that $\delta\hat{W}_h$ of [5], which assumes an isotropic slowing down distribution function and static plasma, is approximately a further $2^{1/2}$ too small when compared with $\delta\hat{W}_h$ in Fig. 4 for $\Delta\lambda \to \infty$. Such a differential has also been observed in recent NOVA-K calculations [40]. The exact semi-analytical approach employed in the present paper enables an explanation for the error in the simplified analytical formula employed in Refs. [5] and [15]. Assuming a static plasma and isotropic hot distribution function ($\Delta\Omega_E = 0$ and $\Delta\lambda \to \infty$) it is clear that $\delta\hat{W}_{hk}$ in Ref. [15] is identical to the expression given in Eq. (18) with the parameter values $q = 1$, $s = 0$ and $\eta = 0$. The most serious loss of accuracy occurs as a result of $s = 0$, which in effect increases the magnitude of $\langle\omega_{mdh}\rangle$ from the correct expression given by Eq. (A14). For most large tokamak discharges, it is typically found that $0.15 < s_1 < 0.5$, such that setting $s = 0$ reduces $\delta W_{hk} \sim 1/\langle\omega_{mdh}\rangle$ by up to twenty five percent. Ignoring finite pressure amplifies this trend through the dependence of $\langle\omega_{mdh}\rangle$ on $\eta = -2R_0 q^2 \mu_0 (d\langle P\rangle/dr)/B_0^2$. Hence, for meaningful comparisons with tokamak data it is argued that an accurate definition for $\langle\omega_{mdh}\rangle$ should be employed, and the Cauchy principal

19

value of the pitch angle integrals evaluated carefully.

V. DISCUSSION

Research into the effects of fast ions on tokamak instabilities continues to be of importance for interpretation of experimental data, and prediction of the effects of alpha particles in ITER. Theoretical studies into the effects of ICRH or NBI ions on the internal kink mode have tended to concentrate on the stabilizing role of trapped ions, which can be identified as a kinetic addition to the energy principle potential energy. In this respect the present paper advances recent investigations into NBI stabilization of JET sawtoothing plasmas [15,32]. In addition to identifying an accurate expression for the kinetic response of fast ions, the present paper accounts for the effect that unbalanced NBI has on the equilibrium. In particular, the work generalizes the equilibrium to be weakly anisotropic and flowing.

The combined effects of plasma rotation and anisotropy are important for analyzing NBI sawtoothing discharges. In particular, strongly sheared toroidal plasma rotation of up to 30 kHz has been measured in JET [11], and the differing injection angles of many tokamaks gives rise to different degrees of plasma anisotropy. Numerical results are obtained in this paper upon employing a typical JET equilibrium and a distribution function which models the 80 keV Octant 4 NBI system. The distribution function adheres to 'slowing down' in absolute velocity and permits a central pitch angle, governed by the injection angle, and a variable pitch angle width controls focusing. The TRANSP code [36] assists in parameterizing the distribution function. For the model distribution which best describes JET NBI scenarios, where the beam injection is approximately 45°, it is shown that in the absence of plasma rotation the anisotropic fluid term is as stabilizing to the ideal internal kink mode as the kinetic term. The stabilizing role of passing ions, highlighted in Ref. [4] although often ignored in similar studies, is seen to be fundamental. This would be even more evident for scenarios where the injection angle approaches azimuthal, which is seen to be a possible effective means of stabilizing sawteeth.

The possible role of anisotropy for the destabilization of the ideal internal kink mode was first highlighted by Mikhailovskii [10]. However, the present paper demonstrates that any realistic distribution of hot ions is strongly stabilizing to the zero frequency $\tilde{\omega} = 0$ internal kink mode upon inclusion of kinetic effects and the poloidal dependence of the hot ion pressure components. In addition it is seen that the total hot ion response $\delta \hat{W}_h = \delta \hat{W}_{hf} + \delta \hat{W}_{hk}$ varies

only moderately with respect to anisotropy. However this observation does not follow in general when toroidal plasma rotation is taken into account. It is seen that counter rotation of realistic amplitude and shear can significantly reduce kinetic stabilization. This is found to be partly because conservation of the third adiabatic invariant Φ requires $\omega_{*pi} \ll \langle\omega_{mdh}\rangle + \Delta\Omega_E$, which is harder to satisfy for sheared counter rotation ($\Delta\Omega_E < 0$) than for static plasmas. This could help to explain JET discharges [14] (e.g. discharge 8419) which show that the switching on of counter injected NBI coincides with much smaller and more irregular sawteeth than in the Ohmic phase. In contrast it is clear that sheared co-rotation assists in the conservation of Φ. Nevertheless co-rotation can also reduce kinetic stability. This can be understood by noting that $\delta\hat{W}_{hk}$ contains the ratio $(\omega_{*h} + \Delta\Omega_E - \tilde{\omega})/(\langle\omega_{mdh}\rangle + \Delta\Omega_E - \tilde{\omega})$ which decreases from $\sim \epsilon^{-1}$ to ~ 1 as $\Delta\Omega_E$ is increased from zero to a frequency much greater than $\langle\omega_{mdh}\rangle$. Furthermore, the internal kink mode is increasingly sensitive to changes in the plasma rotation for increasing $A_h = \langle P_{h\perp}\rangle / \langle P_{h\parallel}\rangle$. The stability analysis of scenarios corresponding to those employed in JET and PDX highlight this. The NBI sawtoothing discharges in JET are expected to be only moderately sensitive to differing plasma rotation, since for the Octant 4 NBI system it is found that $A_h \approx 0.7$. This can be explained by noting that for such a regime the dominant passing fraction of ions strongly stabilize hot fluid potential energy terms, and these terms are independent of plasma rotation. In contrast, an injection angle equivalent to that used in the PDX experiment yields $A_h \sim 2$, and the resulting dominant trapped fraction significantly reduces hot ion stabilization of the kink mode when plasma rotation is taken into account.

The kinetic contribution employed in this paper is also compared with the widely used analytical expression for slowing down alphas defined in the complete sawtooth model [5]. Recently, the latter expression has been employed to model the kinetic response of NBI in JET [15]. For the cases detailed it is found that the kinetic expression employed in the present paper is larger than that of Ref. [15] by a factor of 1.4 in the limit of isotropy, and $\langle\omega_{mdh}\rangle \gg (\tilde{\omega}, \Delta\Omega_E)$. The difference in values is found to be principally due to employing an accurate expression for $\langle\omega_{mdh}\rangle$ in the present paper which includes the effect of finite shear. However, it is important to note that the shear also enters the internal kink dispersion relation through the ideal growth rate $\gamma_I = -\epsilon_1^2 3^{1/2}\pi\tau_A^{-1}\delta\hat{W}s_1^{-1}$. In contrast to the present paper, this s_1^{-1} dependence is included in the normalization of the δW expressions of Ref. [5]. The s_1^{-1} variation of γ_I has been shown [15] to be fundamental to triggering the onset of sawteeth in NBI discharges in JET. For high power discharges the relevant corresponding

internal kink instability threshold is found to be that of the resistive mode [33,5]: $\gamma_I > -\hat{\rho}/\tau_A$, where τ_A is the toroidal Alfvén time and $\hat{\rho}$ the ion Larmor radius normalized with r_1. For typical values of the shear, the s_1^{-1} variation in γ_I is more important than the variation of $\langle \omega_{mdh}(s) \rangle$ during the ramping of the shear prior to the sawtooth crash.

It is of particular interest to consider why sawteeth are generally smaller when heated with NBI than with ICRH. One important reason that emerges from the present paper is linked to that of Ref. [4] which highlighted the importance of the relative size of the magnetic precessional drift $\langle \omega_{mdh} \rangle$. Taking JET for example where the plasma rotation is usually in the co-current direction and typically 15kHz in NBI heated plasmas, it is found that the differential rotation $\Delta\Omega_E$ is similar in size to $\langle \omega_{mdh} \rangle$, and collectively much greater than $\tilde{\omega}$. Consequently this ordering reduces the ratio $(\omega_{*h} + \Delta\Omega_E - \tilde{\omega})/(\langle \omega_{mdh} \rangle + \Delta\Omega_E - \tilde{\omega})$, relative to that for ICRH minority plasmas which is of the order $\omega_{*h}/\langle \omega_{mdh} \rangle \sim \epsilon_1^{-1}$. The latter follows because ICRH ions are much more energetic than those of NBI such that if any differential plasma rotation exists it will be ignorable compared to the toroidal magnetic drift precession frequency. Perhaps more importantly, the trapped fraction of ICRH minority ions is much greater than the trapped fraction of NBI ions. While predominantly passing ion populations have been shown to be stabilizing to the internal kink mode, populations with large trapped fractions stabilize more effectively in static plasmas. The net effects of anisotropy and plasma rotation can result in δW_h being a factor of two smaller for the case of NBI than for ICRH. This is indicated by comparing $\delta \hat{W}_h$ in Fig. 7 (a) with $\Delta\lambda = 0.5$ and $\Omega_{E0} = 15$ kHz for the case of NBI with that of Fig. 7 (b) with $\Delta\lambda = 0.5$ and $\Delta\Omega_E = 0$ for ICRH. This assumes that Eq. (13) with $\lambda_0 = 0.94$ and $\Delta\lambda = 0.5$ can be considered an approximate representation of the ICRH fast ion distribution function, and that $\langle P_h(r) \rangle$ for NBI and ICRH are identical. In reality the large fast ion pressure gradients usually obtained in the localised heating scheme of ICRH can further inflate the effectiveness of sawtooth stabilisation. The following parameter, defined similarly to $\beta_p(r_1)$, can be used as a measure of the fast particle contributions of contrasting heating schemes:

$$\beta_h = -\frac{2\mu_0}{B_0^2 \epsilon_1^2} \int_0^{r_1} dr \left(\frac{r}{r_1}\right)^{3/2} \frac{\partial \langle P_h \rangle}{\partial r},$$

where $\delta \hat{W}_h = \beta_h/(3\pi(2\epsilon_1)^{1/2})$ for $q = 1$, $s = 0$, $\eta = 0$, $\langle \omega_{mdh} \rangle \gg \tilde{\omega} - \Delta\Omega_E$ and an arbitrary isotropic distribution function.

The analysis presented in this paper has been made tractable by deploying inevitable approximations such as an expansion in the inverse aspect ratio. It is important to point

out that the empirically relevant quantity is the local inverse aspect ratio at the inversion radius, which is in general much smaller than unity. Moreover, unlike the toroidal and shaping contributions to the internal kink mode potential energy, the kinetic and anisotropic fluid contributions do not depend sensitively on the detailed structure of the eigenfunction, which itself is resolved only by taking into account toroidal and shaping effects [20,21]. Another reasonable approximation is the assumption of zero orbit widths for the NBI ions. It is noted however that an investigation into the stabilizing role of more energetic particles such as alpha or ICRH populations requires finite orbit widths to be taken into account. Finally, further study would self-consistently solve the dispersion relation for modes away from marginal stability and look at the effect of plasma rotation on fishbones.

In summary, the anisotropic fluid contribution to the internal kink mode is stabilizing for predominantly passing populations ($P_{h\parallel} \gg P_{h\perp}$) and destabilizing for predominantly trapped populations ($P_{h\perp} \gg P_{h\parallel}$). As a consequence the total fast ion response including the zero frequency kinetic contribution [4] is found to vary only moderately with respect to anisotropy. For the NBI distribution of JET where $P_{h\perp}/P_{h\parallel} \approx 0.7$ the anisotropic fluid contribution is as large as the kinetic contribution, and the total fast ion response is around seventy five percent of that which would be obtained for $P_{h\perp}/P_{h\parallel} \gg 1$. Both co and counter toroidal plasma rotation with differential frequency $|\Delta\Omega_E| \sim \langle\omega_{mdh}\rangle$ can significantly reduce the kinetic contribution to stability. It is seen that counter-rotation has the greatest effect by impeding the conservation of the third adiabatic invariant [4]. However, the anisotropic fluid contribution is unaffected, and as a result the effect of plasma rotation is most important for near-perpendicular injection whereby $P_{h\perp} \gg P_{h\parallel}$. For the case of JET where the injection angle is around $45°$, typical co-rotation frequencies of around 15 - 20 kHz reduce only moderately the fast ion contribution to stability. While toroidal plasma rotation will not significantly modify the fast ion response of particles more energetic than those of NBI, anisotropy is clearly a relevant feature of both NBI and ICRH. However, that the fast particle contribution to the internal kink mode is only moderately sensitive to anisotropy encourages employing auxiliary heated ions to predict the effects of isotropic alpha particles in ITER.

ACKNOWLEDGMENTS

APPENDIX A: KINETIC AND ANISOTROPIC FLUID POTENTIAL ENERGY TERMS

The following expressions for the contributions to δW are valid for any distribution function $F_j(\mathcal{E}, \alpha, r)$. It is usual that only the minority fast ion species are distributed anisotropically, and for this reason the fluid terms described below are written in terms of F_h. However, if the core plasma is also anisotropic, the total anisotropic fluid expression of Eq. (7) is given by $\delta W_{fA} = \sum_j \delta W_{jf}$, where in this case j could denote electrons, thermal ions and fast ions.

As discussed in Sec. II the hot fluid contribution δW_{hf} and Mikhailovskii's [10] corresponding approximate definition δW_{hf}^M are defined respectively in Eqs. (12) and (8). The radial integral contained in δW_{hf}^M can be integrated by parts so that it depends on $\left\langle P_{h\perp} + P_{h\parallel} + C \right\rangle$ and not its derivative. If $\langle P_h \rangle \equiv \left\langle P_{h\perp} + P_{h\parallel} \right\rangle / 2$ is a parameter of the distribution function, Eq. (8) requires only $\langle C_h \rangle$ to be evaluated. On defining the pitch angles $k^2 = (1 - \alpha B_0(1 - \epsilon))/2\alpha B_0 \epsilon$ for trapped ions and $y^2 = 1/k^2$ for passing ions, the distribution function can be written as $F_h(\mathcal{E}, k^2, r)$ or $F_h(\mathcal{E}, y^2, r)$. To leading order in ϵ the poloidal orbit average of C_h can be written:

$$\langle C_h \rangle = -20 m_h \int_0^\infty d\mathcal{E}\, \mathcal{E}^{3/2} \left[\int_0^1 dk^2 \frac{\epsilon^{1/2} K(k^2) F_h(\mathcal{E}, k^2, r)}{[1 + \epsilon(2k^2 - 1)]^{7/2}} + \int_0^1 dy^2 \frac{\epsilon^{1/2} y^4 K(y^2) F_h(\mathcal{E}, y^2, r)}{[y^2 + \epsilon(2 - y^2)]^{7/2}} \right].$$
(A1)

Note that for an isotropic distribution (for which $P_h = (2^{7/2}/3)\pi m_h \int d\mathcal{E}\, \mathcal{E}^{3/2} F_h$) the contents of the square bracket of Eq. (A1) is $2^{5/2}\pi/15$ for diminishing ϵ. It is then clear that $C_h = -2P_h$ and hence $\delta W_{hf}^M = 0$ as required. If $\langle P_h \rangle$ is not a parameter of the distribution function then it is possible to evaluate $\langle P_{h\perp} \rangle$ and $\left\langle P_{h\parallel} \right\rangle$ in a similar way to that of Eq. (A1).

The anisotropic fluid term of Eq. (12) can be written as:

$$\delta W_{hf} = 2^{3/2}\pi^2 m_h B_0 R_0^2 \left(\frac{\xi_0}{R_0} \right)^2 \int_0^{r_1} dr\, r \int_0^\infty d\mathcal{E}\, \mathcal{E}^{3/2} \int_0^{1/B_{\min}} d\alpha \left. \frac{\partial F_h(\mathcal{E}, \alpha, r)}{\partial r} \right|_{\mathcal{E}, \mu} [2I_1 + I_2],$$
(A2)

24

where the partial radial derivative in F_h must be for constant $\mathcal{E}$ and μ (and hence α), not for constant $\mathcal{E}$ and k^2. In addition I_1 corresponds to the contribution from the parallel pressure, and I_2 from the perpendicular pressure. I_1 and I_2 are defined as follows:

$$I_1 = \oint d\theta \left(\frac{B}{B_0}\right) \cos\theta \sqrt{1-\alpha B} \quad \text{and} \quad I_2 = \oint d\theta \left(\frac{B}{B_0}\right) \cos\theta \frac{\alpha B}{\sqrt{1-\alpha B}}. \tag{A3}$$

The pitch angle integral for trapped ions is defined in terms of k^2 with the result

$$\delta W_{hf}^t = 2^{5/2}\pi^2 m_h R_0 \left(\frac{\xi_0}{R_0}\right)^2 \int_0^{r_1} dr\, r^2 \int_0^\infty d\mathcal{E}\,\mathcal{E}^{3/2} \int_0^1 dk^2 \frac{2I_1^t(\epsilon,k^2)+I_2^t(\epsilon,k^2)}{[1+\epsilon(2k^2-1)]^2} \left.\frac{\partial F_h(\mathcal{E},k^2,r)}{\partial r}\right|_{\mathcal{E},\mu}. \tag{A4}$$

The poloidal integrals of I_1^t and I_2^t are evaluated upon expanding in ϵ. The resulting terms involve integrals of the type $\int_0^{\pi/2} d\phi \sin^n\phi\sqrt{1-y^2\sin^2\phi}$ and $\int_0^{\pi/2} d\phi \sin^n\phi/\sqrt{1-y^2\sin^2\phi}$, where n is an even integer, which in turn can be written explicitly in terms of complete elliptic integrals of the first and second kind [37]. The result is:

$$I_i^t(\epsilon,k^2) = \frac{2}{[1+\epsilon(2k^2-1)]^{1/2}} \left(\frac{2}{\epsilon}\right)^{1/2} G_i^t(k^2,r), \tag{A5}$$

where 'i' denotes 1 or 2 and

$$G_1^t(\epsilon,k^2) = \left(\frac{2\epsilon}{3}\right) \left[(1-k^2)K(k^2)+(2k^2-1)E(k^2)\right] + 0(\epsilon^2), \tag{A6}$$

$$G_2^t(\epsilon,k^2) = 2E(k^2) - K(k^2) + \left(\frac{2\epsilon}{3}\right) \left[(1-4k^2)K(k^2)+(8k^2-4)E(k^2)\right] + 0(\epsilon^2). \tag{A7}$$

The pitch angle integral for passing ions can be written in terms of y^2 with the result

$$\delta W_{hf}^p = 2^{5/2}\pi^2 m_h R_0 \left(\frac{\xi_0}{R_0}\right)^2 \int_0^{r_1} dr\, r^2 \int_0^\infty d\mathcal{E}\,\mathcal{E}^{3/2} \int_0^1 dy^2 \frac{2I_1^p(\epsilon,y^2)+I_2^p(\epsilon,y^2)}{[y^2+\epsilon(2-y^2)]^2} \left.\frac{\partial F_h(\mathcal{E},y^2,r)}{\partial r}\right|_{\mathcal{E},\mu}. \tag{A8}$$

Expanding I_1^p and I_2^p in ϵ gives:

$$I_i^p(\epsilon,y^2) = \frac{2}{[y^2+\epsilon(2-y^2)]^{1/2}} \left(\frac{2}{\epsilon}\right)^{1/2} G_i^p(y^2,r), \tag{A9}$$

where 'i' denotes 1 or 2 and

$$G_1^p(\epsilon,y^2) = \left(\frac{2\epsilon}{3y^2}\right) \left[(2-y^2)E(y^2)-2(1-y^2)K(y^2)\right]$$
$$- \left(\frac{2\epsilon^2}{15y^4}\right) \left[(4y^4-12y^2+8)K(y^2)+\left(7y^4+8y^2-8\right)E(y^2)\right], \tag{A10}$$

$$G_2^p(\epsilon,y^2) = 2E(y^2)+(y^2-2)K(y^2) - \left(\frac{2\epsilon}{3y^2}\right) \left[\left(3y^4-8y^2+8\right)K(y^2)+\left(4y^2-8\right)E(y^2)\right]$$
$$- \left(\frac{2\epsilon^2}{15y^4}\right) \left[16(y^4-3y^2+2)K(y^2)-2(y^4-16y^2+16)E(y^2)\right]. \tag{A11}$$

25

Equations (A10) and (A11) are exact given that $B = B_0(1 - \epsilon \cos\theta)$. Due to the range of pitch angles allowed (y^2 can be small), it is found that in order to obtain δW_{hf}^p to reasonable accuracy, all the terms in Eqs. (A10) and (A11) are required for equilibria with realistic ϵ_1. This is especially evident when comparing δW_{hf}^p and δW_{hf}^t which should be equal in magnitude but opposite in sign if an isotropic distribution function is chosen.

Finally, the kinetic contribution to the internal kink mode is considered. Only trapped particles appear. In terms of the pitch angle k^2, Eq. (11) can be written

$$\delta W_{hk} = -2^{7/2}\pi^3 m_h \left(\frac{\xi_0}{R_0}\right)^2 \int_0^{r_1} dr\, r^2 \int_0^1 dk^2\, \frac{I_q^2}{K_b} \int_0^\infty d\mathcal{E}\, \mathcal{E}^{5/2} \frac{\partial F_h}{\partial \mathcal{E}} \left[\frac{\omega_{*h} + \Delta\Omega_E - \tilde{\omega}}{\langle \omega_{mdh}\rangle + \Delta\Omega_E - \tilde{\omega}}\right], \tag{A12}$$

where $K_b = (2/\epsilon)^{1/2}\pi^{-1}K(k^2)$ and $I_q = (2/\epsilon)^{1/2}\pi^{-1}\mathcal{F}_q$ with

$$\mathcal{F}_q = \int_0^{\pi/2} d\phi \frac{\cos[2q \arcsin(k \sin\phi)]}{\sqrt{1 - k^2\sin^2\phi}}. \tag{A13}$$

The hot ion diamagnetic and magnetic drift frequencies are defined:

$$\omega_{*h} = \frac{m_h q}{ZeB_0 r}\frac{\partial F_h/\partial r}{\partial F_h/\partial \mathcal{E}} \quad \text{and} \quad \langle \omega_{mdh}\rangle = \frac{m_h q \mathcal{E}}{ZeB_0 R_0 r}\left[\mathcal{F}_1 + 2s\mathcal{F}_2 - \eta\left(\frac{1}{4q^2} + \mathcal{F}_3\right)\right], \tag{A14}$$

where again the partial derivative in $\mathcal{E}$ is for constant μ (not k^2). The effect of finite shear arises through $s = d\ln q/d\ln r$ and finite beta effects [41] through $\eta = -2R_0 q^2 \mu_0 (d\langle P\rangle/dr)/B_0^2$, with $\langle P\rangle$ the total plasma pressure. The functions $\mathcal{F}_{1,2,3}$ are defined accurately in terms of elliptic integrals in Ref. [13]. Also contained in the latter reference is a fit of $\mathcal{F}_q$, also in terms of elliptic integrals, which is very accurate within the range $0 < k^2 < 1$ and $0.5 < q < 1$. For $q = 1$, $s = 0$, $\eta = 0$, $\tilde{\omega} = 0$ and $\Delta\Omega_E = 0$, it can be seen that δW_{hk} cancels with δW_{hf}^t of Eq. (A4) if only the leading order term of $G_1^t + G_2^t$ in Eq. (A7) is retained. The remaining hot ion contribution to the kink mode then comes from δW_{hf}^p which is stabilizing to the kink mode, especially for predominately passing populations.

[1] D. J. Campbell, D. F. H. Start, J. A. Wesson, D. V. Bartlett *et al*, Phys. Rev. Lett. **60** 2148 (1988).

[2] C. K. Phillips J. Hosea, E. Marmar, M. W. Phillips *et al*, Phys. Fluids B **4**, 2155 (1992).

[3] D. J. Campbell, L. Baylor, V. P. Bhatnagar, M. Bures *et al*, *Proceedings of Contributed Papers*, 15th European Physical Society Conference on Controlled Fusion and Plasma Heating, Dubrovnik, 1988 (European Physical Society, Petit-Lancy, 1989), p. 377.

[4] F. Porcelli, Plasma Phys. Controlled Fusion **33**, 1601 (1991).

[5] F. Porcelli, D. Boucher and M. N. Rosenbluth, Plasma Phys. Controlled Fusion **38**, 2163 (1996).

[6] O. Sauter, E. Westerhof, M. L. Mayoral, B. Alper *et al*, Phys. Rev. Lett. **88**, 105001 (2002).

[7] J. Wesson, *Tokamaks*, 2nd ed. (Oxford Science Publications, Oxford, 1997), p. 581.

[8] T. G. Northrop, *The Adiabatic Motion of Charged Particles* (Interscience, New York, 1963), p. 61.

[9] A. B. Mikhailovskii, Sov. J. Plasma Phys **8**, 477 (1983).

[10] A. B. Mikhailovskii, Sov. J. Plasma Phys **9**, 190 (1983).

[11] D. Testa, C. Giroud, A. Fasoli and K. -D. Zastrow, Physics of Plasmas **9** 243 (2002).

[12] F. L. Waelbroeck, Phys. Plasmas **3**, 1047 (1996); C. Wahlberg and A. Bondeson, Phys. Plasmas **7**, 923 (2000); R. G. Kleva and P. N. Guzdar, Phys. Plasmas **9**, 3013 (2002).

[13] J. P. Graves, R. J. Hastie and K. I. Hopcraft, Plasma Phys. Contol. Fusion **42**, 1049 (2000).

[14] D. J. Campbell, Private Communication, 2000.

[15] C. Angioni, A. Pochelon, N. N. Gorelenkov, K. G. McClements *et al*, Plasma Phys. Control. Fusion **44**, 205 (2002).

[16] B. Coppi, R. Galvao, R. Pellat, M. N. Rosenbluth and P. H. Rutherford, Sov. J. Plasma Phys. **2**, 533 (1976).

[17] G. F. Chew, M. L. Goldberger and F. E. Low, Proc. R. Soc. London, **A236**, 112 (1956).

[18] J. B. Taylor and R. J. Hastie, Phys. Fluids **8**, 323 (1965).

[19] V. D. Shafranov, Sov. Phys. Tech. Phys. **15**, 175 (1970).

[20] M. N. Bussac, R. Pellat, D. Edery and J. L. Soulé, Phys. Rev. Lett. **35**, 1638 (1975).

[21] D. Edery, G. Laval, R. Pellat and J. L. Soulé, Phys. Fluids **19**, 260 (1976).

[22] N. A. Madden and R. J. Hastie, Nucl. Fusion **34**, 519 (1994).

[23] J. P. Graves, K. I. Hopcraft, R. O. Dendy, R. J. Hastie *et al*, Phys. Rev. Lett. **84**, 1204 (2000).

[24] A. B. Mikhailovskii, *Instabilities in a Confined Plasma*, (IOP Publishing, London, 1998), p. 276.

[25] K. G. McClements, R. O. Dendy, R. J. Hastie and T. J. Martin, Phys. Plasmas **3**, 2994 (1996).

[26] J. W. Connor, S. C. Cowley, R. J. Hastie and L. R. Pan, Plasma Phys. and Control. Fusion **29**, 919 (1987).

[27] H. F. Tammen, A. J. H. Donné, H. Euringer and T. Oyevaar, Phys. Rev. Lett. **72**, 356 (1994).

[28] L. Chen, R. B. White and M. N. Rosenbluth, Phys. Rev. Lett. **52**, 1122 (1984).

[29] M. F. F. Nave, N. N. Gorelenkov, K. G. McClements, S. J. Allfrey *et al*, Nucl. Fusion **42**, 281 (2002).

[30] M. D. Kruskal and C. R. Oberman, Phys. Fluids **1**, 275 (1958).

[31] H. L. Berk, W. Horton, M. N. Rosenbluth and P. H. Rosenbluth, Nucl. Fusion **15**, 819 (1975).

[32] N. N. Gorelenkov, M. F. F. Nave, R. Budny, C. Z. Cheng *et al*, *Proceedings of Contributed Papers*, 27th European Physical Society Conference on Controlled Fusion and Plasma Physics, Budapest, 2000 (European Physical Society, Petit-Lancy, 2000), p. 1553.

[33] B. Coppi, S. Migliuolo, F. Pegoraro and F. Porcelli, Phys. Plasmas B **2**, 927 (1990).

[34] K. G. McClements, R. O. Dendy, C. G. Gimblett, R. J. Hastie and T. J. Martin, Nucl. Fusion **35**, 1761 (1995).

[35] F. Pegoraro, B. Coppi, P. Detragiache and S. Migiuolo, *Proceedings of Contributed Papers*, 12th International Atomic Energy Agency Conference on Plasma Physics and Controlled Nuclear Fusion Research, Nice, 1988 (IAEA, Vienna, 1989), Vol. 2, p. 243.

[36] R. Budny, Nucl. Fusion **34**, 1247 (1994).

[37] M. Abramowitz and I. A. Stegun, *Handbook of Mathematical Functions*, (Dover Publications, Inc., New York, 1965), p. 590.

[38] K. McGuire, R. Goldston, M. Bell, M. Bitter and K. Bol *et al*, Phys. Rev. Lett. **50**, 891 (1983).

[39] R. O. Dendy, R. J. Hastie, K. G. McClements and T. J. Martin, Phys. Plasmas **2**, 1623 (1995).

[40] S. C. Jardin, C. E. Kessel, D. Meade, J. Breslau *et al*, *Proceedings of Contributed Papers*, 29th European Physical Society Conference on Plasma Physics and Controlled Fusion, Montreux, 2002 (European Physical Society, Petit-Lancy, 2002), p. 1.084.

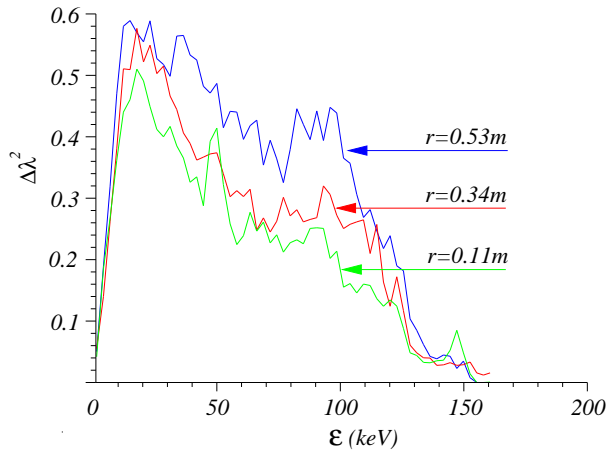[41] J. W. Connor, R. J. Hastie and T. J. Martin, Nucl. Fusion **23**, 1702 (1983).

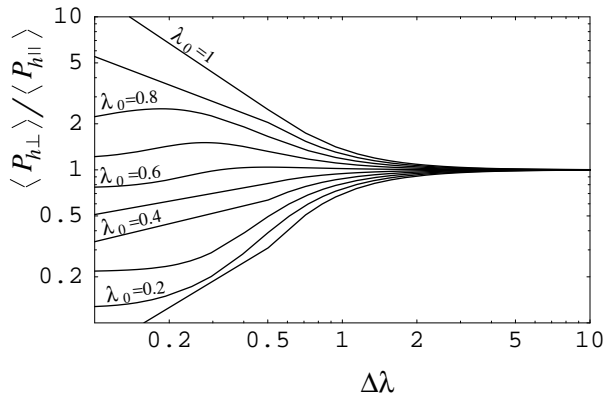FIG. 1. Showing the square of the pitch angle width versus energy for different minor radius.

FIG. 2. Log-Log plot showing a measure of anisotropy $A_h = \langle P_{h\perp} \rangle / \langle P_{h\parallel} \rangle$ versus pitch angle width $\Delta\lambda$ for different central pitch angles λ_0. A small inverse aspect ratio is chosen for these curves, although A_h does not change sensitively with respect to ϵ. It is seen that the isotropic limit $A_h = 1$ is approximately reached for $\Delta\lambda > 2$ regardless of λ_0.
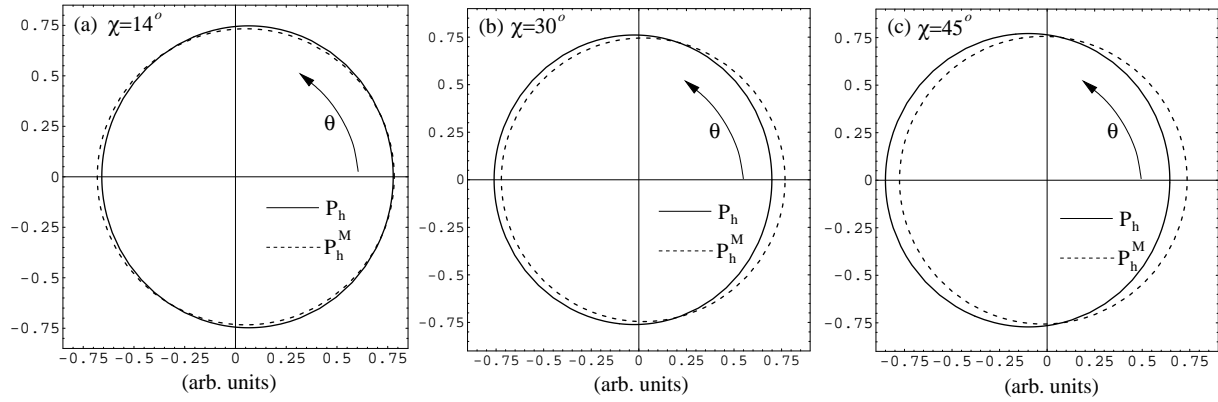
FIG. 3. Polar plots of P_h and P_h^M with arbitrary units of magnitude. The angular variable in the plot is θ, and the pitch angle width is chosen to be $\Delta\lambda = 0.5$. (a) is for an injection angle of $14°$ ($\lambda_0 = 0.94$), (b) is for $\chi = 30°$ ($\lambda_0 = 0.75$) and (c) is for $\chi = 45°$ ($\lambda_0 = 0.5$).
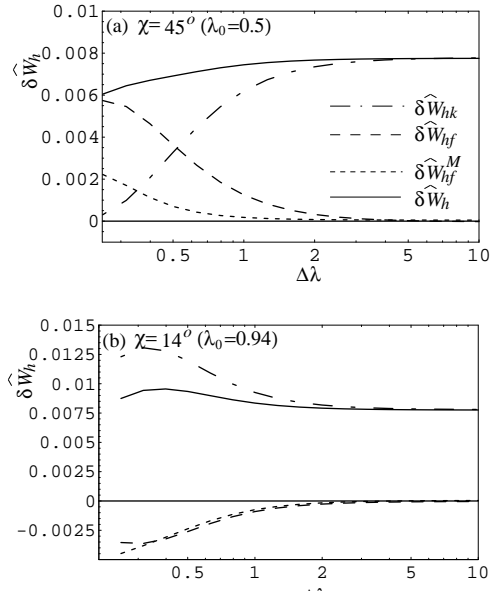
FIG. 4. Log-linear plots of the distinct components of the hot ion potential energy $\delta\hat{W}_h = \delta\hat{W}_{hf} + \delta\hat{W}_{hk}$ together with $\delta\hat{W}_{hf}^M$ as a function of the pitch angle width $\Delta\lambda$: (a) is for injection angle $\chi = 45°$ ($\lambda_0 = 0.5$) and (b) is for $\chi = 14°$ ($\lambda_0 = 0.94$). The degree of anisotropy A_h corresponding to λ_0 and $\Delta\lambda$ can be observed in Fig. 2.
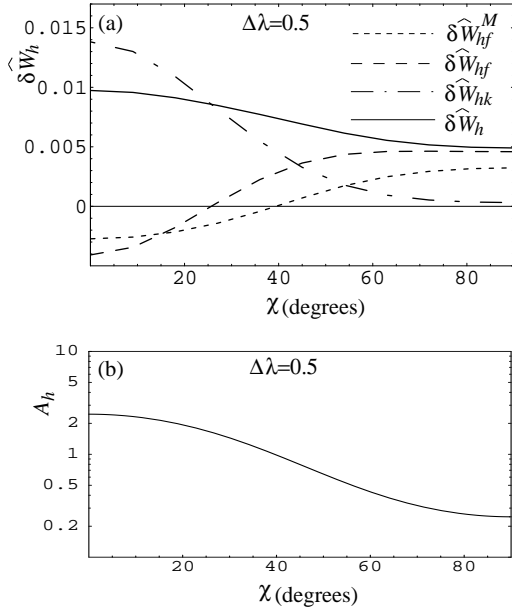
FIG. 5. (a) Showing $\delta\hat{W}_h$, $\delta\hat{W}_{hk}$, $\delta\hat{W}_{hf}$ and $\delta\hat{W}_{hf}^M$ as a function of χ for $\Delta\lambda = 0.5$. (b) Depicts a linear-log plot of the corresponding degree of anisotropy A_h.
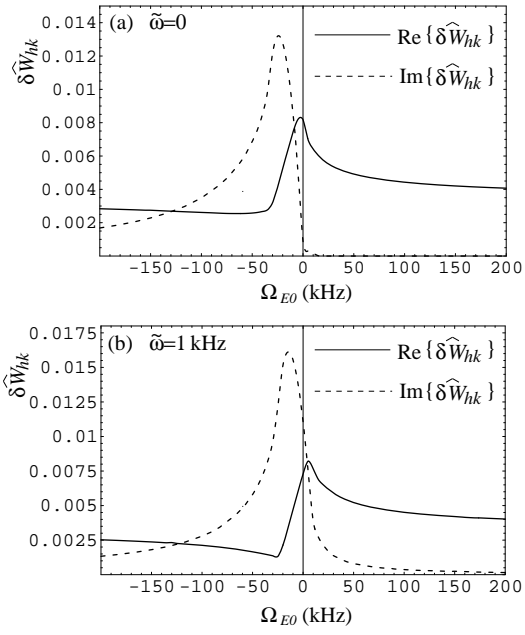
FIG. 6. Showing the real and imaginary components of $\delta\hat{W}_{hk}$ for a very large range of central toroidal plasma rotation Ω_{E0} and for an isotropic distribution function ($\Delta\lambda \to \infty$). (a) is for mode frequency $\tilde{\omega} = 0$ and (b) is for $\tilde{\omega} = 1$ kHz.
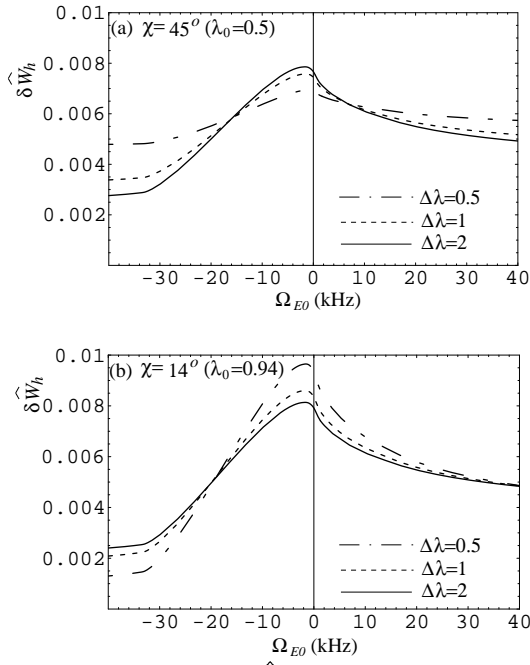
FIG. 7. Plots of $\delta\hat{W}_h$ with respect to the central toroidal plasma rotation Ω_{E0} for three different pitch angle widths. (a) is for $\chi = 45°$ ($\lambda_0 = 0.5$) and (b) is for $\chi = 14°$ ($\lambda_0 = 0.94$).